tert-Butyl(trifluoromethyl)tellurium: A Novel Organometallic Chemical Vapor Deposition Source for ZnTe

Michal Danek, Sanjay Patnaik,† and Klavs F. Jensen*

Department of Chemical Engineering, Massachusetts Institute of Technology, Cambridge, Massachusetts 02139

Douglas C. Gordon, Duncan W. Brown, and Rein U. Kirss‡

Advanced Technology Materials, 7 Commerce Drive, Danbury, Connecticut 06810

Received March 23, 1993. Revised Manuscript Received June 25, 1993®

tert-Butyl(trifluoromethyl)tellurium, *t*-BuTeCF$_3$, a novel organometallic chemical vapor deposition source with high vapor pressure and low decompostion temperature, has been used in combination with dimethylzinc to deposit ZnTe in the temperature range 280–550 °C. Films synthesized below 400 °C were heavily contaminated with ZnF_2 crystallites ranging in size from 1 to 20 μm, depending upon the Te/Zn ratio and growth temperature. Above 400 °C, relatively pure ZnTe films were grown. Corresponding growth curves, measured *in situ* with a microbalance, exhibited a reduction of growth rate at the transition from ZnTe/ZnF_2 to pure ZnTe. Growth with bis(trifluoromethyl)tellurium, $(CF_3)_2Te$, yielded ZnTe films without fluorine incorporation, but the growth rate was low even at 500 °C. Pyrolysis of *t*-BuTeCF$_3$ in hydrogen and helium was studied by molecular beam mass spectroscopy at reduced pressure. A decomposition mechanism consistent with the experimental observations is proposed. Decomposition begins at 230 °C and occurs *via* two competing pathways: β-hydrogen elimination and homolysis of the *tert*-butyl–Te bond. A high isobutene-to-isobutane ratio in the pyrolysis products suggests that β-hydrogen elimination prevails over homolysis in the temperature range 250–450 °C. Unstable (trifluoromethyl)tellurol, the primary product of β-hydrogen elimination, decomposes to difluorocarbene, tellurium, and hydrogen fluoride. The difluorocarbene reacts with isobutene to yield 1,1-difluoro-2,2-dimethylcyclopropane or undergoes dimerization to tetrafluoroethene. The hydrogen fluoride reacts with dimethylzinc and leads to the ZnF_2 contamination.

Introduction

The combination of a direct bandgap of 2.26 eV (at room temperature) and its naturally p-type character make ZnTe a promising material for optoelectronic devices operating in the blue-green region.[1] To reduce the density of intrinsic defects, control stoichiometry, and minimize dopant diffusion across heterojunctions, a low growth temperature of ZnTe films is desirable. ZnTe films have been grown previously by organometallic chemical vapor deposition (OMCVD) using either dimethyl- or diethylzinc and various tellurium organometallic sources. The thermal stability and consequently, the growth temperature obtained with these sources, correlate with the stability of the corresponding radicals generated by homolysis of the Te–alkyl bond, and the accessibility of other decomposition pathways, such as β-hydrogen elimination. Tellurium–alkyl bond dissociation enthalpy decreases in the order methyl > primary alkyl > secondary alkyl > tertiary alkyl > allyl. Thus, dimethyltellurium (DMTe) and diethyltellurium (DETe) decompose at high temperatures, and OMCVD growth of ZnTe films with these sources has been carried out at temperatures typically above 450 and 410 °C, respectively.[2] Diisopropyltellurium (DIPTe) has been used for ZnTe growth at 350 °C.[3] Diallyltellurium (DATe), di-*tert*-butyltellurium (DTBTe), and methylallyltellurium (MATe) have made growth of CdTe and $Hg_{1-x}Cd_xTe$ (MCT) possible below 300 °C.[4] However, the low decomposition temperature is accompanied by low vapor pressures, which reduce the delivery rate of the sources and growth rate of the films.[5]

Unsymmetrical (trifluoromethyl)alkyltellurium compounds, CF_3TeR (R = *tert*-butyl or benzyl), were recently proposed as new OMCVD sources.[6] These sources were designed to achieve a low decomposition temperature and optimal vapor pressure and to maintain good stability at room temperature. The trifluoromethyl group reduces intermolecular interactions, resulting in a significant increase in the vapor pressure of the sources compared to

† Presently at International Paper, Corporate Research Center, Tuxedo, NY 10987.

‡ Presently at Department of Chemistry, Northeastern University, Boston, MA 02115.

® Abstract published in *Advance ACS Abstracts*, August 15, 1993.

(1) (a) Kobayashi, M.; Dosho, S.; Imai, A.; Konagai, M.; Takahashi, K. *Appl. Phys. Lett.* **1987**, *51*, 1602. (b) Jackson, M. K.; Miles, R. H.; McGill, T. C.; Faurie, J. P. *Appl. Phys. Lett.* **1989**, *55*, 786. (c) Tarasawa, T.; Ohkawa, K.; Mitsuyu, T. *Appl. Phys. Lett.* **1989**, *54*, 117. (d) Kumazaki, K.; Iida, F.; Ohno, K.; Hatano, K.; Imai, K. *J. Cryst. Growth* **1992**, *117*, 285. (e) Lee, D.; Johnson, A. M.; Zucker, J. E.; Burrus, C. A.; Feldman, R. D.; Austin, R. F. *Appl. Phys. Lett.* **1992**, *60*, 739.

(2) (a) Wilson, B. A.; Bonner, C. E.; Feldman, R. D.; Austin, R. F.; Kisker, D. W.; Krajewski, J. J.; Bridenbaugh, P. M. *J. Appl. Phys.* **1988**, *64*, 3210. (b) Ogawa, H.; Mitsuhiro, N. *J. Appl. Phys.* **1988**, *64*, 6750. (c) Mitsuhiro, N.; Ogawa, H. *Jpn. J. Appl. Phys.* **1990**, *29*, 145. Yokogawa, T.; Narusawa, T. *Appl. Phys. Lett.* **1992**, *61*, 291.

(3) (a) Wagner, H. P.; Kuhn, W.; Gebhardt, W. *J. Cryst. Growth* **1990**, *101*, 199. (b) Mullins, J. T.; Clifton, P. A.; Brown, P. D.; Brinkman, A. W.; Woods, J. *J. Cryst. Growth* **1990**, *101*, 100.

(4) Pain, G. N.; Christiansz, G. I.; Dickson, R. S.; Deacon, G. B.; West, B. O.; McGregor, K.; Rowe, R. s. *Polyhedron* **1990**, *9*, 921 and references therein.

(5) Hails, J. E.; Irvine, S. J. C.; Mullin, J. B. *Mater. Res. Soc. Symp. Proc.* **1990**, *161*, 343.

(6) Gordon, D. C.; Kirss, R. U.; Brown, D. W. *Organometallics* **1992**, *11*, 2947.

0897-4756/93/2805-1321$04.00/0

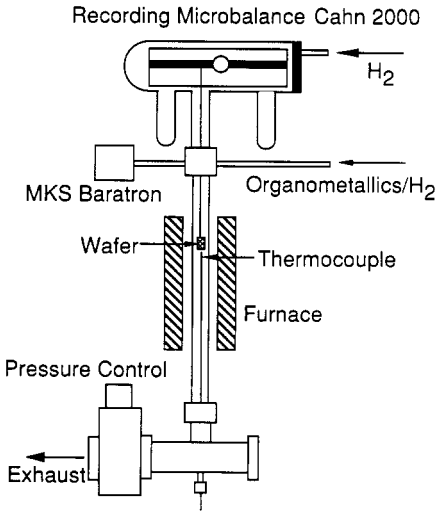

Figure 1. Microbalance system.

Table I. Vapor Pressure of Tellurium OMCVD Sources at 20 °C

source	vapor pressure at 20 °C, Torr
dimethyltellurium[4]	40.7
diethyltellurium,[4]	7.1
diisopropyltellurium[5]	2.6
di-*tert*-butyltellurium[5]	1.6
diallyltellurium[5]	1.1
methylallyltellurium[5]	4.5
tert-butyl-trifluoromethyltellurium	17.8
bis(trifluoromethyl)tellurium	531

the other reagents (Table I). Since *tert*-butyl or benzyl groups form more stable free radicals, the sources were expected to decompose at a low temperature by Te–R bond homolysis. However, pyrolysis studies in a hot tube showed that the decomposition of the *tert*-butyl derivative was complete at 335 °C, while the benzyl derivative required 450 °C.[6] This behavior was explained in terms of β-hydrogen elimination as an alternative decomposition pathway for the *tert*-butyl compound.

Here we present an OMCVD growth study of ZnTe with *tert*-butyl (trifluoromethyl)tellurium, *t*-BuTeCF$_3$. Since the composition of grown films with the *tert*-butyl compound suggests a complex reaction mechanism involving C–F bond activation, we also discuss investigations of the pyrolysis of *t*-BuTeCF$_3$ at growth conditions in a molecular beam mass spectrometer (MBMS) system. In addition, results from growth with bis(trifluoromethyl)-tellurium, $(CF_3)_2Te$, another high vapor pressure compound (Table I), are included to provide insight into the role of the Te–CF$_3$ moiety in fluorine contamination of ZnTe.

Experimental Section

Material. *tert*-Butyl(trifluoromethyl)tellurium and bis(trifluoromethyl)tellurium were prepared at Advanced Technology Materials by previously described procedures.[6] Dimethylzinc and ultrahigh-purity argon were supplied by Air Products, and ultrahigh-purity hydrogen and high-purity helium by Matheson. Isobutane and isobutene were obtained from Aldrich and used as received. Zinc-doped GaAs(100) wafers were supplied from Crystal Specialties. All reagents used for wafer preparation were of electronic grade.

OMCVD Growth. The growth experiments were conducted in a hot-wall tubular reactor equipped with a Cahn 2000 microbalance system for monitoring the growth rate *in situ* (Figure 1). GaAs(100) wafers were degreased in boiling 1,1,2-trichloroethylene and acetone. Then the wafers were etched in HCl and in a mixture of sulfuric acid, hydrogen peroxide, and deionized water in a volume ratio of 5:1:1. A controlled oxide layer was grown in deionized water and etched in HCl. Finally, the wafers were thoroughly rinsed with isopropyl alcohol and immediately loaded into the reactor. Before growth, the wafers were baked in hydrogen flow at 160–170 °C for several hours. The delivery rate of DMZn was 20 μmol/min, while the delivery rate of *t*-BuTeCF$_3$ was varied from 5 to 50 μmol/min. In the growth experiments with $(CF_3)_2Te$, the delivery rate of the tellurium source was kept at 20 μmol/min. The reactor pressure was maintained at 10 Torr by a Vacuum General pressure regulator (Model 80-2) and total carrier gas flow rate was 25 standard cubic centimeters per minute (sccm). Several growth rate measurements at varying temperatures and Te/Zn ratios were carried out on one sample. The growth rate at one reference point was monitored during every run to detect any significant deterioration of the sample quality. Because of the composition changes in the films at temperatures below 420 °C, the high-temperature portion of growth curves was measured first on each sample.

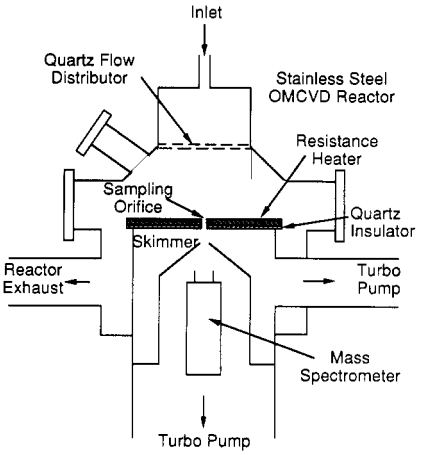

Figure 2. Molecular beam mass spectrometer (MBMS) system.

Film Characterization. Several samples with film thickness from 2 to 20 μm were prepared for characterization. The crystallinity of the films was inspected by X-ray diffraction on a rotating anode Rigaku 300 diffractometer using monochromatized Cu Kα radiation. A Perkin-Elmer Auger scanning microprobe (Model 660) was used for analysis of the film composition. Surface morphology was observed on a Cambridge scanning electron microscope (Model 250 Mk 3). Secondary ion mass spectrometer (VG Ionex, Ltd., Cs^+ primary beam) was used for estimation of the fluorine content in the films grown from *t*-BuTeCF$_3$ at 400 °C and from $(CF_3)_2Te$ at 500 °C.

Pyrolysis of *t*-BuTeCF$_3$ in the Molecular Beam Mass Spectrometer (MBMS) System. The MBMS system is schematically shown in Figure 2, and it has been described in detail elsewhere.[7] The tellurium source was pyrolyzed in hydrogen or helium in a stagnation point flow reactor stage. The gas phase in the vicinity of the graphite resistance heater was sampled through a 100-μm orifice in a 25-μm stainless steel foil into a high-vacuum stage pumped by a Leybold-Heraeus 450 turbomolecular pump. The expanded molecular beam was extracted by a skimmer into the second stage, differently pumped with a Leybold-Heraeus 360 turbomolecular pump, and analyzed with a Balzers 311 quadrupole mass spectrometer. In a typical experiment, 20 μmol/min of *t*-BuTeCF$_3$ were carried in 25 sccm of hydrogen or helium into the reactor. Reactor pressure was maintained at 30 Torr. To correct the spectra for sampling flux at various heater temperatures, 0.4 sccm of argon was flowed with the carrier gas into the reactor. The mass spectra were scaled based upon the Ar^+ signal; the contribution from the fragmentation pattern of the parent was subtracted from the corrected data. In trapping experiments, approximately a 10-fold excess of isobutene was flowed together with *t*-BuTeCF$_3$ into the MBMS system.

(7) (a) Lee, P. W.; Omstead, T. R.; McKenna, D. R.; Jensen, K. F. *J. Cryst. Growth* **1987**, *85*, 165. (b) Lee, P. W.; Omstead, T. R.; McKenna, D. R.; Jensen, K. F. *J. Cryst. Growth* **1988**, *93*, 29.

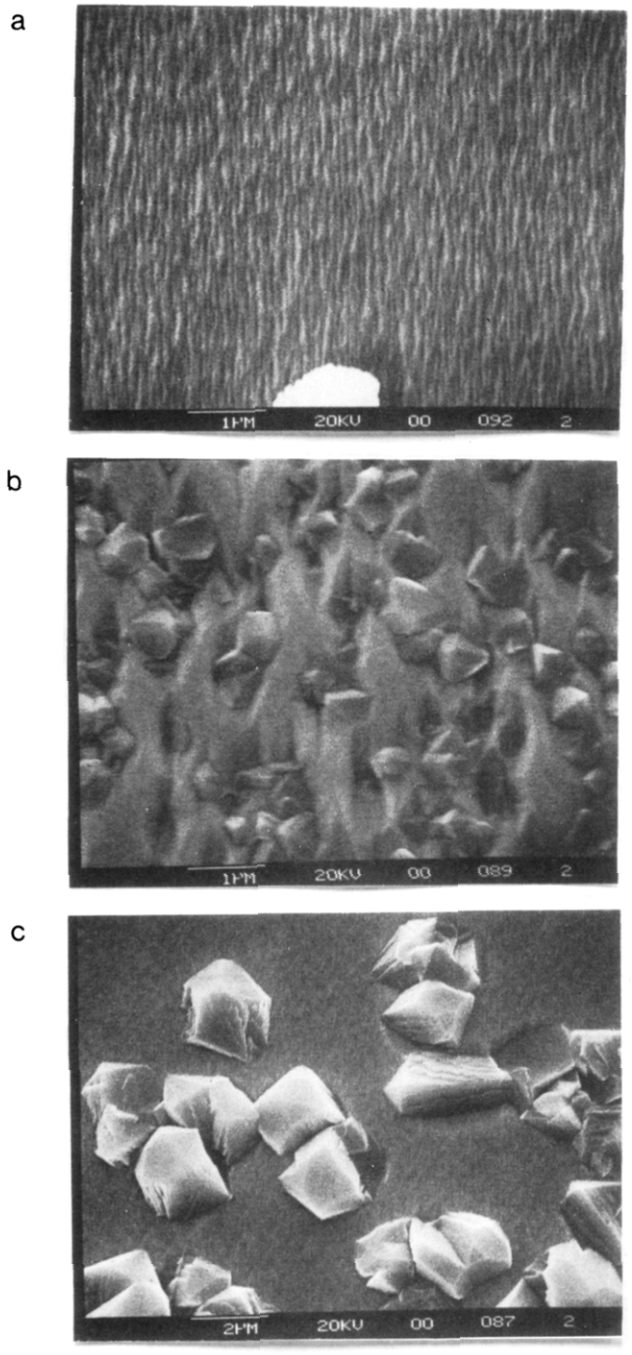

Figure 3. SEM micrographs of films grown from t-$BuTeCF_3$ at various substrate temperatures at Te/Zn = 1.0. (a) 400, (b) 350, and (c) 300 °C.

Results and Discussion

Growth of ZnTe. The OMCVD growth experiments showed that the morphology and composition of the films had a strong dependence on the growth temperature and Te/Zn ratio. The SEM micrographs on Figure 3 illustrate the effect of growth temperature. At temperatures above 400 °C, the grown layers were relatively smooth with characteristic ridges (Figure 3a). In contrast, the films deposited at 350 °C contained surface defects caused by the incorporation of a large number of submicron crystallites (Figure 3b). When the growth temperature was reduced, the crystallites became larger and more scattered (Figure 3c). At constant growth temperature, the crystalline dimensions decreased and the density of the coverage increased with increasing Te/Zn ratio. This effect is shown in Figure 4 for growth temperature of 350 °C. At

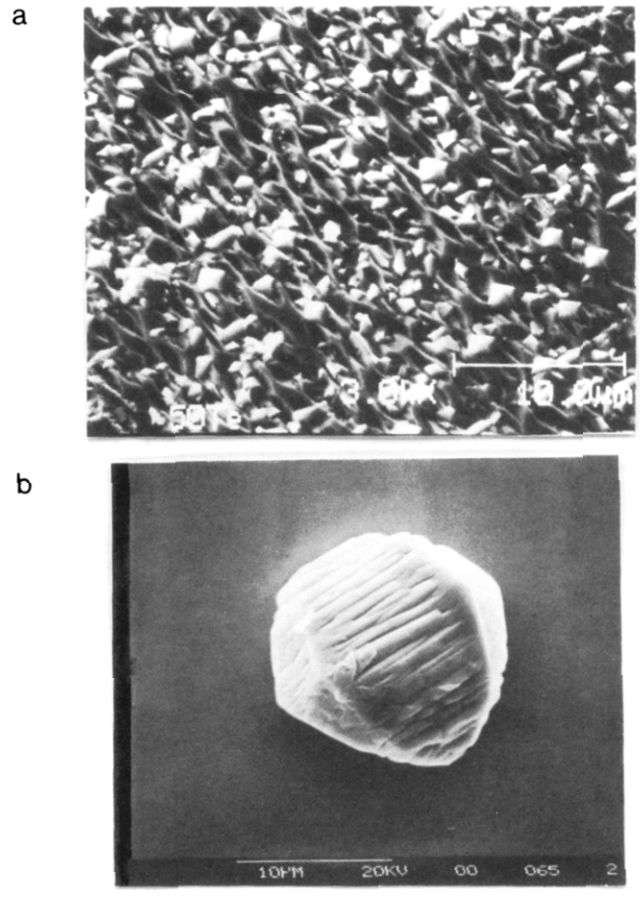

Figure 4. SEM micrographs of films grown from t-$BuTeCF_3$ at various Te/Zn ratios at 350 °C: (a) 2.5 and (b) 0.25.

a high Te/Zn ratio, the crystallite size was typically below 1 μm and the coverages were very dense (Figure 4a), while at a ratio of 0.25, the size exceeded 10 μm and the crystallites was scarce (Figure 4b). The layer below the large crystallites (Figures 3c and 4b) was smooth and almost featureless.

The Auger spectrum of the film grown at 400 °C (Figure 5a) contained peaks corresponding to zinc, tellurium, oxygen, and carbon. The latter two signals disappeared after short sputtering by Ar^+, which indicates postgrowth contamination when the samples were exposed to air. The content of fluorine in the film was below the detection limit of the Auger spectrometer.[8] The film grown at 350 °C with a high coverage of crystallites contained zinc, tellurium, and fluorine (Figure 5b). The Auger spectra showed that the dominant constituents of the large crystallites in the films grown below 400 °C, and at low Te/Zn ratio, are zinc and fluorine (Figure 5c). The underlying smooth layer consisted of zinc and tellurium, without any detectable contamination of fluorine by Auger (Figure 5d). Additional analysis of the film grown at 400 °C by SIMS revealed a high fluorine content in the range approximately 10^{18}–10^{20} atoms/cm^3. The fluorine contamination is segregated into islands, several micrometers large, with fluorine concentrations one to two orders of magnitude higher than the surrounding matrix (Figure 6); the tellurium density remains uniform.

The diffraction patterns from the films grown in the temperature range from 300 to 400 °C at a Te/Zn ratio of 1.0 are shown in Figure 7. All the grown ZnTe layers were highly oriented in the ⟨100⟩ direction. The position of

(8) AES detection limit of fluorine at our conditions was approximately 0.1–0.2 atom %.

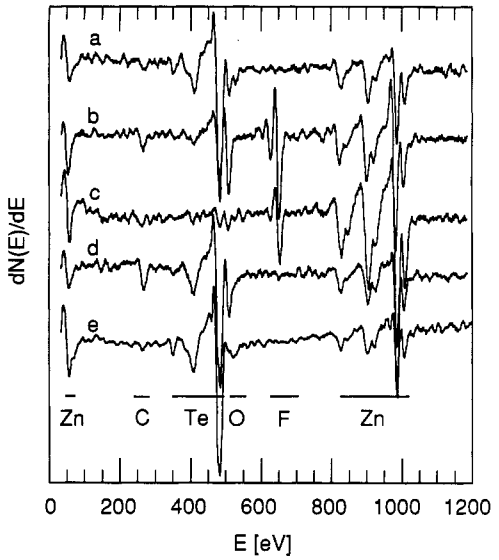

Figure 5. Auger electron spectra of films grown at Te/Zn = 1.0. (a) film from *t*-BuTeCF$_3$ at 400 °C (surface sputtered); (b) film with crystallites from *t*-BuTeCF$_3$ at 350 °C; (c) crystallite on film from *t*-BuTeCF$_3$ at 300 °C; (d) film between crystallites from *t*-BuTeCF$_3$ at 300 °C, and (e) film from $(CF_3)_2Te$ at 500 °C (surface sputtered).

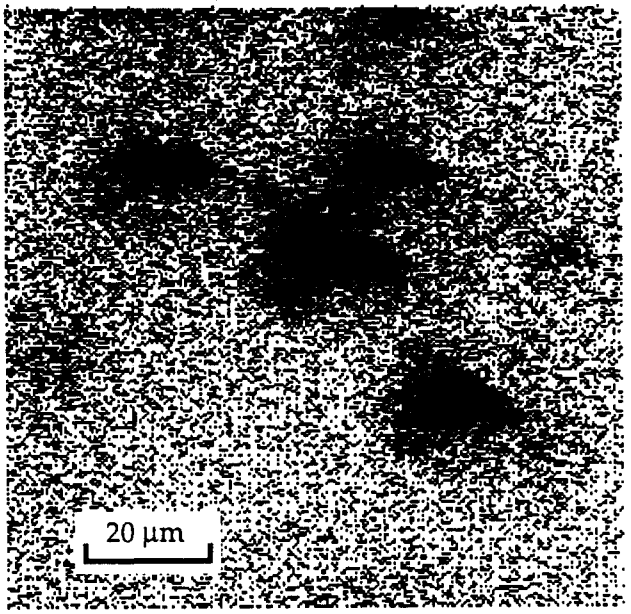

Figure 6. SIMS fluorine map of film from *t*-BuTeCF$_3$ at 400 °C. Black color indicates an elevated fluorine content.

the (400) line corresponds to the bulk lattice parameter, indicating that the films are already relaxed.[1d,9] The (111) diffraction in the patterns suggests a presence of misoriented domains that might have their origin in the large lattice mismatch (7.8% at room temperature). The diffraction pattern of the films grown at 300 and 350 °C (Figure 7b,c) contained very weak diffraction lines from ZnF_2. The relative intensity of the lines suggests a preferred orientation of the crystallites in the ⟨001⟩ direction.

Corresponding to the film composition, there were two distinct regions in the temperature dependence of the growth rate as is shown in Figure 8. The low-temperature region, where the films were contaminated with ZnF_2 crystallites, is characterized by an apparent activation

(9) Kudlek, G.; Presser, N.; Gutowski, J.; Hingerl, K.; Abramof, E.; Pesek, A.; Pauli, H.; Sitter, H. *J. Cryst. Growth* **1992**, *117*, 290.

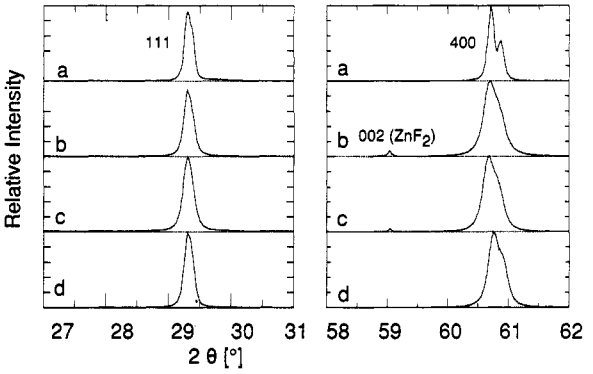

Figure 7. X-ray diffraction of films grown at Te/Zn = 1.0. (a) film from *t*-BuTeCF$_3$ at 400 °C; (b) film from *t*-BuTeCF$_3$ at 350 °C; (c) film from *t*-BuTeCF$_3$ at 300 °C; (d) film from $(CF_3)_2Te$ at 500 °C.

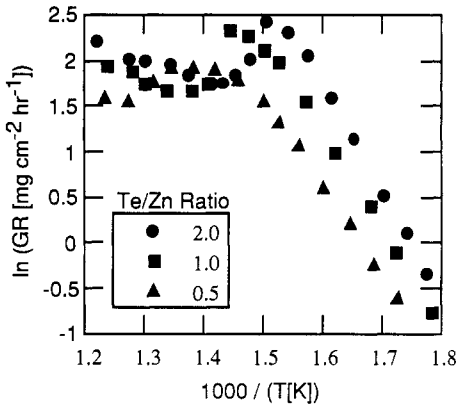

Figure 8. Arrhenius plot for growth from *t*-BuTeCF$_3$ at Te/Zn equals 2.0 (●), 1.0 (■), and 0.5 (▲).

energy of 23 kcal/mol. The growth rate increased with the increase of the Te/Zn ratio. The low-temperature region ends with a sharp drop of the growth rate in the temperature range 375–420 °C, depending upon the Te/Zn ratio. Above this transition temperature, the growth rate varied only slightly with substrate temperature and the films were not contaminated with ZnF_2 crystallites. The mechanism of the transition is not clear, but the character of the contamination indicates that the nucleation of ZnF_2 on a growing ZnTe film played an important role. At a high ZnTe growth rate, the nucleation of ZnF_2 may be too slow for the formation of the crystallites. Also, the absence of ZnF_2 phase at high temperatures possibly could be attributed to the equilibrium

$$ZnF_2 + TeR_2 \rightleftarrows ZnTe + 2RF$$

being shifted to the right-hand side. However, thermodynamic calculations based upon estimated quantities for the Te/Zn compounds show the equilibrium to be far to the ZnF_2 side. This conclusion is relatively insensitive to errors in estimates of the thermodynamic data for TeR_2.

The growth rate in the high-temperature region also depended upon the Te/Zn ratio and this behavior is illustrated in Figure 9 for a growth temperature of 440 °C. For ratios below 0.5, the zinc source was rate limiting. The growth rate reached a maximum at a Te/Zn of 0.6 and was followed by a decrease at higher Zn/Te ratios. This phenomenon could be rationalized by the presence of a parasitic reaction depleting DMZn. Estimates of the mass-transfer rate based upon the reactor and sample geometry indicated that the measured growth rate was well below the diffusion limit.

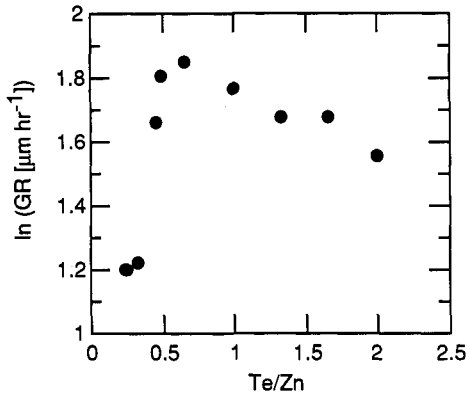

Figure 9. Growth rate of ZnTe growth from t-BuTeCF$_3$ at 440 °C at various Te/Zn ratios.

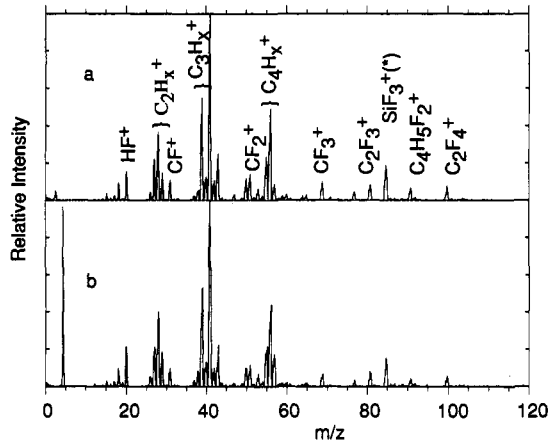

Figure 10. MBMS spectra of t-BuTeCF$_3$ pyrolyzed (a) in dihydrogen at a heater temperature of 398 °C; (b) in helium at 412 °C. The major peaks of the products are assigned. The peak denoted by an asterisk is observed only above the decomposition temperature of the source and may have its origin in the reaction of HF with the quartz insulating plate of the MBMS heater.

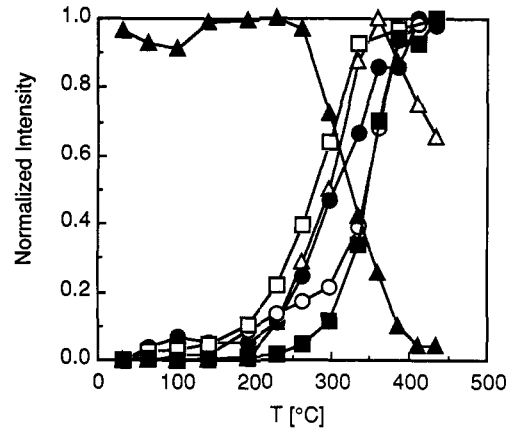

Figure 11. Pyrolysis of t-BuTeCF$_3$ in H$_2$ at 30 Torr. Normalized mass spectrometer intensies for species in the gas phase as a function of heater temperatures. The following symbols are used: ▲ parent; □ isobutene (m/z = 56); ○ isobutane (m/z = 43); ● hydrogen-fluoride (m/z = 20); △ tetrafluoroethene (m/z = 100); ■ 1,1-difluoro-2,2-dimethylcyclopropane (m/z = 91).

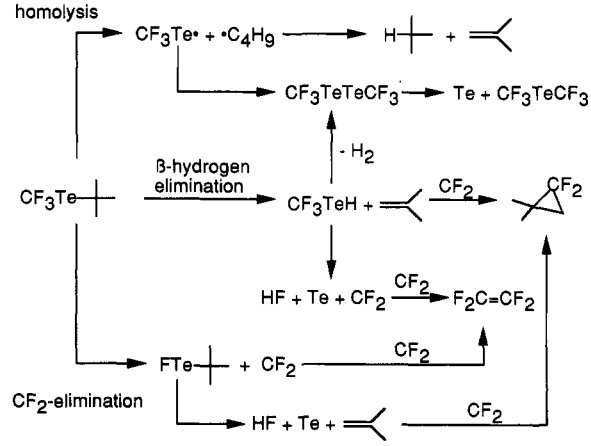

Figure 12. Proposed gas-phase decomposition pathways of t-BuTeCF$_3$.

Since the growth experiments with t-BuTeCF$_3$ pointed toward an unexpected decomposition mechanism involving C–F bond activation and ZnF$_2$ incorporation, OMCVD growth with another (fluoroalkyl)tellurium compound, (CF$_3$)$_2$Te, was explored even though a high decomposition temperature and a high growth temperature were expected, based upon a previous study.[6] Indeed, the growth rate was low, approximately 1 μm/h, even at 500 °C. The film surface was featureless, and the main constituents were zinc and tellurium (Figure 5e). Surprisingly, fluorine was uniformly incorporated into the film at concentrations below 10^{18}–10^{19} atoms/cm^3. The diffraction pattern of a film grown at 500 °C (Figure 7d) is comparable to that for the films grown from t-BuTeCF$_3$ under similar conditions.

Pyrolysis of t-BuTeCF$_3$. To probe the mechanism of ZnF$_2$ formation, a pyrolysis study of t-BuTeCF$_3$ was performed. Mass spectra of the reagent pyrolyzed in dihydrogen and helium at 412 and 398 °C, respectively, are shown in Figure 10. The difference between the pyrolysis in hydrogen and in helium appears to be marginal. The parent molecule decomposes with an apparent activation energy of 32 kcal/mol, and the pyrolysis yields the following dominant products: isobutane, isobutene, hydrogen fluoride, tetrafluoroethene, and 1,1-difluoro-2,2-dimethylcyclopropane. The normalized intensities of mass spectral signals corresponding to the parent and the products are shown in Figure 11 as a function of heater temperature. Starting at low temperatures, the first volatile product is isobutene, generated with the onset of the source decomposition at 230 °C. The generation of isobutene is followed by the formation of hydrogen fluoride and tetrafluoroethene. Isobutane and 1,1-difluoro-2,2-dimethylcyclopropane are formed above 300 °C. The appearance of 1,1-difluoro-2,2-dimethylcyclopropane is accompanied by a drop in tetrafluoroethene concentration, indicating the presence of two competing reaction channels. The decomposition of the parent is complete by 400 °C, but the expected product, (CF$_3$)$_2$Te, is not observed.[6] This suggests that homolytic cleavage of the t-Bu–Te bond may be only a minor decomposition pathway and that under low-pressure conditions, CF$_3$TeH, the primary product of β-hydrogen elimination, does not undergo an intermolecular coupling leading to (CF$_3$)$_2$Te and H$_2$. The same trend in the distribution of the pyrolysis products was found in helium.

On the basis of MBMS data and results from the previous pyrolysis study,[6] we propose three possible pathways for the decomposition of t-BuTeCF$_3$ (Figure 12). The first is homolytic cleavage of the t-Bu–Te bond, yielding (trifluoromethyl)tellurium and *tert*-butyl radicals (pathway a). The CF$_3$Te• radicals are expected to undergo recombination, leading initially to formation of (CF$_3$)$_2$Te$_2$ and eventually to tellurium metal and (CF$_3$)$_2$Te.[6] It is well-known that *tert*-butyl radicals disproportionate to isobutane and isobutene. In the absence of another hydrogen donor, a 1:1 ratio of these products is expected.

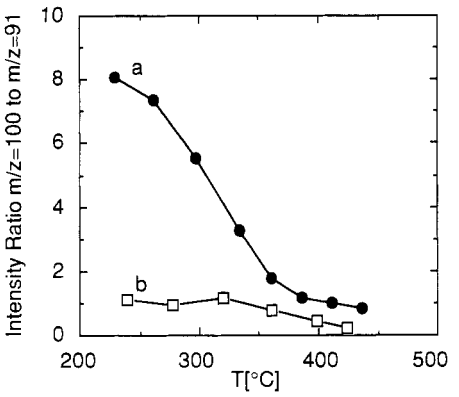

Figure 13. Pyrolysis of t-$BuTeCF_3$. Effect of isobutene addition on the ratio of ion signals at m/z = 100 (tetrafluoroethene) and m/z = 91 (1,1-difluoro-2,2-dimethylcyclopropane): (a) t-$BuTeCF_3$ 20 μmol/min; (b) t-$BuTeCF_3$ 20 μmol/min, isobutene 170 μmol/min.

The second decomposition pathway (b) is β-hydrogen elimination, leading to (trifluoromethyl)tellurol, CF_3TeH, and isobutene. (Trifluoromethyl)tellurol can undergo either bimolecular condensation yielding $(CF_3)_2Te_2$ and H_2 or, more probably at reduced pressure conditions, monomolecular decomposition *via* difluorocarbene extrusion, accompanied by formation of HF and elemental tellurium. Difluorocarbene dimerization and addition to isobutene account for the formation of tetrafluoroethene and 1,1-difluoro-2,2-dimethylcyclopropane. In agreement with this proposal, a trapping experiment, in which excess isobutene was added, showed that the ratio of these products was shifted away from tetrafluoroethene and toward 1,1-difluoro-2,2-dimethylcyclopropane (Figure 13).

The third decomposition pathway (c), which also should be considered,[10] starts with difluorocarbene extrusion yielding *tert*-butyltellurium fluoride, t-BuTeF. If this tellurium intermediate underwent subsequent β-hydrogen elimination, the same pyrolysis products as in the second decomposition pathway would be expected. However, no evidence for t-BuTeF has been observed in the mass spectra. In addition, the high decomposition temperatures of analogous $BzTeCF_3$[6] and CF_3TeCF_3 suggest that difluorocarbene extrusion from $RTeCF_3$ does not occur readily at temperatures below 400 °C.

Theoretically, the relative contribution of β-hydrogen elimination and homolysis should be reflected in the isobutene/isobutane ratio, since the former produces only isobutene, whereas the latter produces a 1:1 ratio of isobutene to isobutane. (The reaction of the *tert*-butyl radical with hydrogen is too slow in the studied temperature range[11] to contribute significantly to the concentration of isobutene.) The ratio of the corresponding partial pressures *vs* decomposition temperature is shown in Figure 14. The ratio has a maximum value at 300 °C and then decreases with increasing temperature; however, its value remains large (>15) at all temperatures. Therefore, though the relative importance of the competing decomposition pathways may change with temperature, the data clearly suggests that β-hydrogen elimination is the *predominant* decomposition pathway for t-$BuTeCF_3$ in the temperature range 250–450 °C.

(10) CF_2 extrusion has been documented in many examples from organometallic chemistry of main group elements—for a review see: Seyferth, D. In *Carbenes II*; Moss, R. A., Eds.; Wiley: New York, 1975; pp 101.

(11) Kondratiev, V. N. In *Rate Constants of Gas Phase Reactions*; Fristrom, R. M., Ed.; NSRDS: 1972.

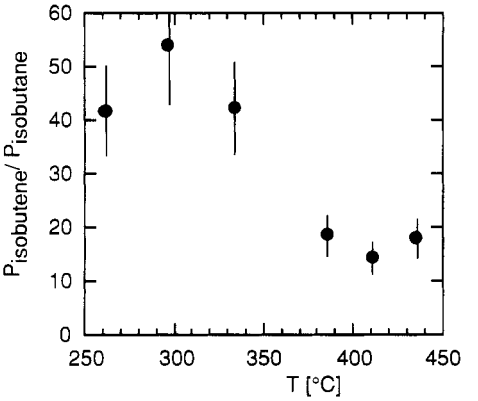

Figure 14. Pyrolysis of t-$BuTeCF_3$. Ratio of isobutene and isobutane partial pressure as a function of heater temperatures.

Hydrogen fluoride is one of the primary pyrolysis products of t-$BuTeCF_3$ and originates, presumably, from unstable CF_3TeH, the primary intermediate of β-hydrogen elimination. Hydrogen fluoride would undergo a rapid gas-phase reaction with DMZn to form ZnF_2, which is observed to contaminate the films at temperatures below 400 °C. Preliminary MBMS studies of the reaction of t-$BuTeCF_3$ with DMZn at the growth conditions showed that formation of free HF was dramatically reduced. In addition, the temperature at which decomposition begins was significantly reduced for both sources, suggesting that gas-phase adduct formation may also play a role in the growth mechanism. An alternative explanation for ZnF_2 formation is alkyl exchange between t-$BuTeCF_3$ and $(CH_3)_2Zn$ to form $(CF_3)_2Zn$, which decomposes to give CF_2 and ZnF_2. An analogous reaction was observed to occur when $(CF_3)_2Te$ was allowed to react with $(CH_3)_2Cd$.[12] Preliminary MBMS experiments have not shown the presence of CF_3TeCH_3 or $(CH_3)_2Te$, which would be the products of alkyl-exchange reactions. Since these products are relatively stable at the temperatures studied and should be detected easily, their absence is a strong indication that alkyl exchange is not important in the ZnF_2 information. A second observation supporting this assertion is the absence of ZnF_2 in films grown from $(CF_3)_2Te$ and DMZn. A detailed study of the gas-phase interaction of t-$BuTeCF_3$ and $(CF_3)_2Zn$ is of future interest in order to fully understand the mechanism of ZnF_2 contamination of ZnTe.

Conclusion

OMCVD growth experiments show that ZnTe can be grown from t-$BuTeCF_3$ at temperatures above 300 °C. Growth in the range of 300–400 °C yields films contaminated with ZnF_2 crystallites, but above 400 °C the films are ZnTe. Films grown with $(CF_3)_2Te$ are without fluorine incorporation, but at the expense of a low growth rate even at 500 °C. On the basis of pyrolysis in a MBMS system, t-$BuTeCF_3$ beings to decompose at 230 °C. The primary decomposition pathway is *via* β-hydrogen elimination, but products originating from *tert*-butyl–tellurium bond homolysis are also observed. The ZnF_2 contamination is believed to originate from the gas-phase reaction of DMZn, with HF formed from the unstable products of β-hydrogen elimination.

Acknowledgment. The financial support of the National Science Foundation is gratefully acknowledged.

(12) Naumann, D.; Lange, H. *J. Fluorine Chem.* **1985**, *27*, 299.